

Supplementary Information

One-step synthesis of highly crystalline covalent organic framework with olefin and imine dual linkages for tuning photocatalytic activity

Qing Sun,^{1, 2} Shaodong Jiang,^{2,4} Hongyun Niu,² Ying Li,⁵ Xiaodong Wu,⁵ Yali Shi,^{1, 2} and Yaqi Cai^{1, 2, 3, 4, *}

¹School of Environment, Hangzhou Institute for Advanced Study, University of Chinese Academy of Sciences, Hangzhou 310024, China

²State Key Laboratory of Environmental Chemistry and Ecotoxicology, Research Center for Eco-Environmental Sciences, Chinese Academy of Sciences, Beijing 100085, China

³Hubei Key Laboratory of Environmental and Health Effects of Persistent Toxic Substances, School of Environment and Health, Jiangnan University, Wuhan 430056, China

⁴University of Chinese Academy of Sciences, Beijing 100049, China

⁵Key Laboratory of Environmental Pollution Control Technology of Zhejiang Province, Eco-Environmental Science Research & Design Institute of Zhejiang Province, Hangzhou 310007, China

*Correspondence: caiyaqi@rcees.ac.cn (Y. Cai).

Table of Contents

Section S1 General Information.....	2
Section S2 Experimental Procedures	3
Section S3 Powder X-ray diffraction analysis	4
Section S4 Structure modeling.....	5
Section S5 Characterization of COFs	9

Section S1 General Information

1.1 Chemicals and reagents

All reagents were purchased from commercial sources and used without further purification.

1,3,5-tris(4-formyl-phenyl)triazine (TFPT) were obtained from Jilin Chinese Academy of Sciences - Yanshen Technology Co., Ltd. (Jilin, China). 1,4-phenylenediamine (PA), anhydrous N,N-dimethylformamide (DMF) were purchased from J&K Scientific Ltd. (Beijing, China). 4-aminophenylacetonitrile (APA) were acquired from Shanghai Aladdin Biochemical Technology Co., Ltd. (Shanghai, China).

1.2 Characterization

Powder X-ray diffraction (PXRD) data were collected from a Bruker D8-ADVANCE diffractometer (Bruker, Germany) using a Cu K α ($\lambda = 1.5418 \text{ \AA}$) radiation ranging from 2° to 30° with a resolution of 0.02° . Fourier transform infrared (FTIR) spectra in the $4000\text{--}400 \text{ cm}^{-1}$ region was recorded on a Nicolet iS10 FTIR spectrometer (Thermo Fisher Scientific, Waltham, MA). Solid-state nuclear magnetic resonance (ssNMR) spectra were obtained on a 600 MHz Bruker Avance III spectrometer (Bruker, Germany). Surface area and pore volume were measured by Brunauer-Emmett-Teller (BET) methods (ASAP2460; Micrometric, Norcross, GA). Thermogravimetric analysis (TGA) curves were recorded on a TGA/DSC 3+ thermal analysis system under N_2 -flow (METTLER TOLEDO, Swiss). The diffuse reflectance spectra (DRS) were collected using a Metash UV-8000 UV-vis spectrophotometer (BaSO_4 as a reflectance standard).

All the electrochemical properties were investigated on a CHI760E electrochemical analyzer (Chenhua, Shanghai, China) in a standard three-electrode system, using a platinum foil as the counter electrode and Saturated Calomel Electrode (SCE) as the reference electrode. The electrolyte was a $0.1 \text{ mol}\cdot\text{L}^{-1} \text{ Na}_2\text{SO}_4$ aqueous solution. The working electrodes were prepared as follows: 5 mg of photocatalyst powder was dispersed in 0.5 mL of ethanol, which was dip-coated on the surface of indium tin oxide (ITO) glass substrate. Subsequently, 5% Nafion-ethanol solution was dripped onto the sample film and dried at room temperature. Mott-Schottky curves were measured at a frequency of 1 kHz. Visible-light irradiation was provided by a CEL-HXF300F3 300 W xenon lamp (CEAULIGHT) with a 420 nm cut-off filter.

1.3 Analysis

The concentration of sulfathiazole was analyzed by using Dionex U3000® HPLC system (Dionex, Sunnyvale, CA) with a UV detector. Sulfathiazole was separated on Dikma C18 column ($5 \mu\text{m}$, $4.6 \text{ mm} \times 150 \text{ mm}$). The mobile phase consisted of acetonitrile/water (20:80) containing 0.06% acetic acid. The wavelength was set at 284 nm, and the flow rate was 1.0 mL min^{-1} with a column temperature of 30°C .

Section S2 Experimental Procedures

Preparation of TFPT-APA COF

A quartz tube measuring 10 × 8 mm (o.d. × i.d.) was charged with 1,3,5-tris(4-formyl-phenyl)triazine (TFPT) (118 mg, 0.3 mmol), 4-aminophenylacetonitrile (APA) (59 mg, 0.45 mmol), 2 mL of DMF, 2 mL of ethanol, and 0.1 mL of piperidine. The tube was flash frozen at 77 K in liquid N₂ bath, degassed by three freeze-pump-thaw cycles, and flame sealed. The reaction was heated at 120 °C for 72 h yielding a red precipitate at the bottom of the tube. The powder was isolated by centrifugation and washed with methanol (25 mL×3), chloroform (15 mL×1) and hexanes (15 mL×1), and dried at room temperature and evacuated under vacuum at 100 °C, 6 h to afford a yellow powder. The average yield from three independent experiments is 79.5%.

Preparation of TFPT-PA COF

A quartz tube measuring 10 × 8 mm (o.d. × i.d.) was charged with 1,3,5-tris(4-formyl-phenyl)triazine (TFPT) (118 mg, 0.3 mmol), 1,4-phenylenediamine (PA) (49 mg, 0.45 mmol), 2 mL of DMF, 2 mL of ethanol, and 0.2 mL of piperidine. The tube was flash frozen at 77 K in liquid N₂ bath, degassed by three freeze-pump-thaw cycles, and flame sealed. The reaction was heated at 120 °C for 72 h yielding a red precipitate at the bottom of the tube. The powder was isolated by centrifugation and washed with methanol (25 mL×3), chloroform (15 mL×1) and hexanes (15 mL×1), and dried at room temperature and evacuated under vacuum at 100 °C, 6 h to afford a yellow powder. The average yield from three independent experiments is 89.3%.

Photocatalytic activity measurements

The photocatalytic activities of the synthesized COFs were evaluated by degradation of crystalline violet (CV), rhodamine B (RB), and sulfathiazole (STZ) under visible light irradiation. The visible light source was a 300 W xenon lamp equipped with an optical cutoff filter ($\lambda \geq 420$ nm). Typically, 15 mg of COF powder was dispersed in a 50 mL aqueous solution containing organic pollutant at a concentration of 10 ppm. Before photocatalytic degradation, the solution was stirred for 1 h or 40 min in the dark to reach an adsorption–desorption equilibrium. For CV and RB, 3 mL aliquots were taken out at certain times and centrifuged to remove the photocatalyst. After that, the resulting supernatants were analyzed by monitoring the absorbance spectra on a UV–vis spectrophotometer. For STZ, 1 mL aliquots were taken out and filtered through 0.22 μ m PES filters to remove the photocatalyst. The filtrate was then analyzed by HPLC to determine the remaining STZ content.

Section S3 Powder X-ray diffraction analysis

Pawley refinements were performed using the Reflex module in Materials Studio. All the patterns were refined using the Pseudo-Voigt function, with all FWHM parameters (U, V, W), profile parameters (NA, NB), and line shift allowed to vary. Lattice parameter were also refined.

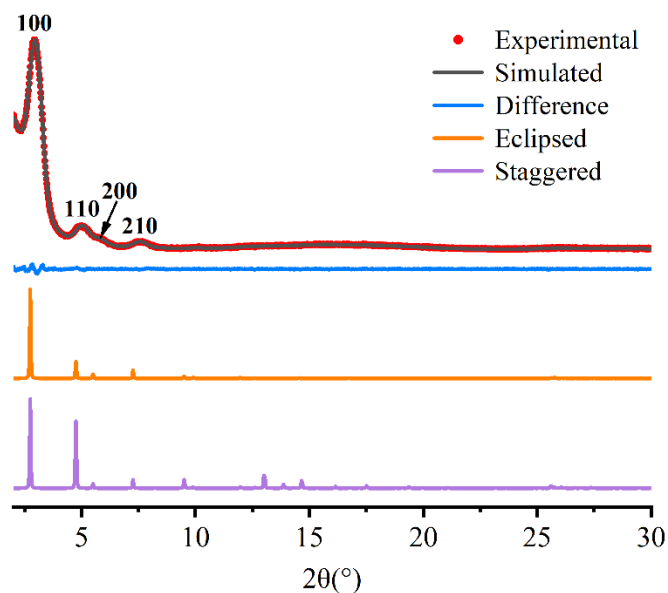


Fig. S1. PXRd patterns of TFPT-PA COF (red pots: experimentally observed, black: Pawley refinement, blue: their difference, orange: simulated with eclipsed mode, purple: simulated with staggered mode.)

Section S4 Structure modeling

Structural models of COFs were generated using the Accelrys Materials Studio 7.0 software package. The proposed model was geometry optimized using the Forcite Module (Universal force fields, Ewald summations) to obtain the optimized lattice parameters.

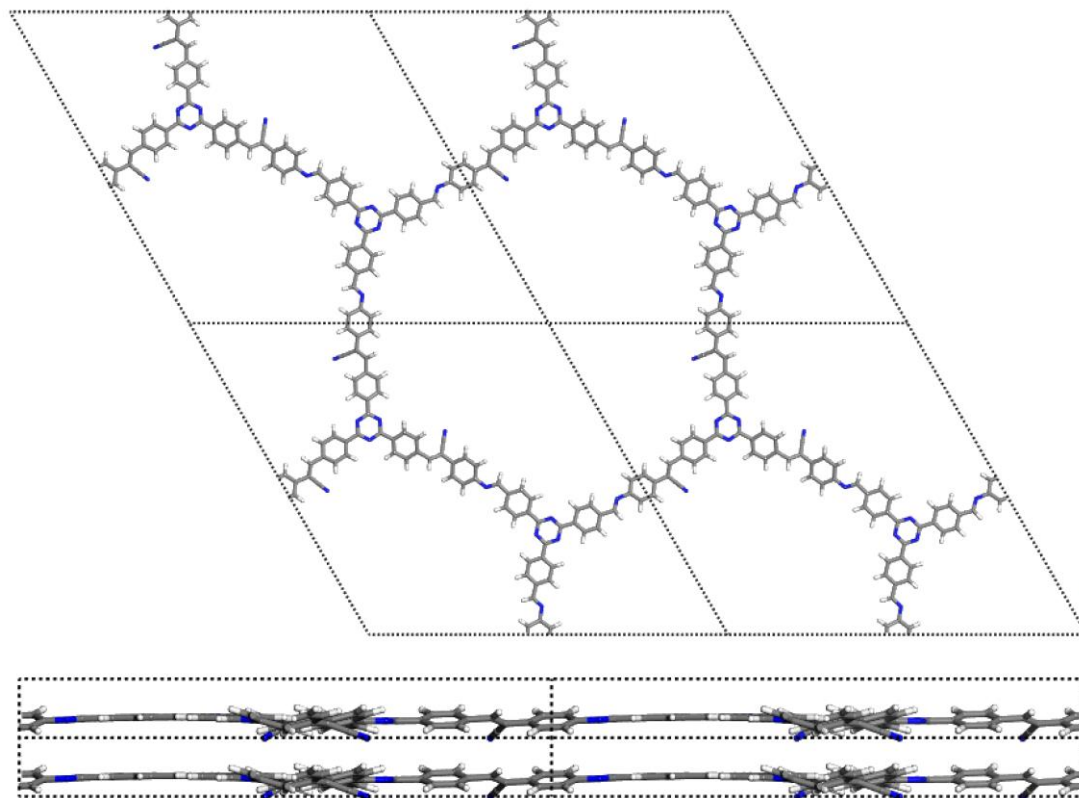


Fig. S2. 2×2×2 cells of TFPT-APA COF from Materials Studio.

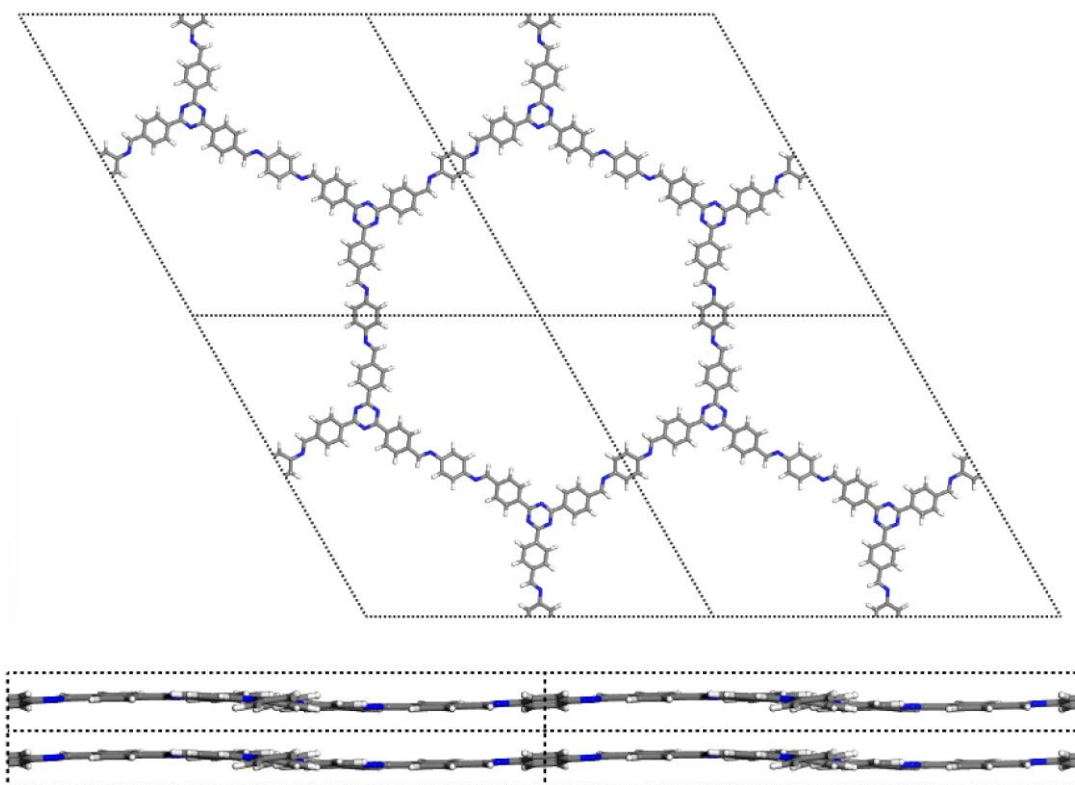


Fig. S3. 2×2×2 cells of TFPT-PA COF from Materials Studio.

Table S1 Atomic coordinates of the Pawley-refined TFPT-APA COF

TFPT-APA, Pawley refined		<i>P3</i> (143)		
$a = b = 36.0942 \text{ \AA}; c = 3.6268 \text{ \AA}$				
$\alpha = \beta = 90^\circ; \gamma = 120^\circ$				
Atom Name	Atom	x	y	z
C1	C	0.41536	0.7786	1.20321
C2	C	0.43499	0.82176	1.21315
C3	C	0.41294	0.84177	1.31048
C4	C	0.37093	0.81758	1.4081
C5	C	0.35114	0.77442	1.39359
C6	C	0.37316	0.75447	1.29178
C7	C	0.35243	0.70877	1.28587
N8	N	0.31048	0.68563	1.28604
C9	C	0.49169	0.57854	0.23915
C10	C	0.51013	0.5513	0.2623
C11	C	0.48698	0.50907	0.1678
C12	C	0.50484	0.48397	0.18569
C13	C	0.4517	0.56405	1.33414
H14	H	0.43312	0.76408	1.12321
H15	H	0.46752	0.83965	1.14227
H16	H	0.35351	0.8316	1.5083
H17	H	0.31885	0.7566	1.47316

H18	H	0.45532	0.49561	0.07134
H19	H	0.48652	0.45159	0.11028
C20	C	0.51773	0.62028	0.10238
C21	C	0.55168	1.56774	0.3712
C22	C	0.56958	1.54263	0.38728
C23	C	0.54626	1.50044	0.29123
N24	N	0.56292	1.47308	0.30348
C25	C	0.60181	1.48388	0.32213
C26	C	0.61459	1.45232	0.33348
C27	C	0.58533	1.40985	0.33438
C28	C	0.59816	1.38053	0.34185
C29	C	0.6405	1.39304	0.34851
C30	C	0.66968	1.43558	0.34927
C31	C	0.65681	1.46488	0.34195
C32	C	0.65413	1.36195	0.35209
N33	N	0.62583	1.32089	0.35197
N34	N	0.53888	1.65368	-0.00575
H35	H	0.43352	0.53224	1.42765
H36	H	0.57023	1.59999	0.44989
H37	H	0.60125	1.55638	0.48192
H38	H	0.62564	1.51613	0.31963
H39	H	0.55251	1.39922	0.32843
H40	H	0.57484	1.34804	0.34122
H41	H	0.70253	1.44634	0.35466
H42	H	0.67992	1.49745	0.34178

Table S2 Atomic coordinates of the Pawley-refined TFPT-PA COF

TFPT-PA, Pawley refined		<i>P3</i> (147)		
$a = b = 37.0182 \text{ \AA}; c = 3.3280 \text{ \AA}$				
$\alpha = \beta = 90^\circ; \gamma = 120^\circ$				
Atom Name	Atom	x	y	z
C1	C	0.43007	0.77153	1.39261
C2	C	0.45633	0.81454	1.39764
C3	C	0.43993	0.84113	1.42516
C4	C	0.3967	0.82398	1.44606
C5	C	0.37042	0.78098	1.44024
C6	C	0.38681	0.75424	1.41424
C7	C	0.35896	0.70864	1.41163
N8	N	0.31711	0.6921	1.41171
N9	N	0.45779	0.54603	0.46329
C10	C	0.47827	0.52201	0.48056
C11	C	0.45704	0.47909	0.55636
C12	C	0.47871	0.45742	0.57252

C13	C	0.4181	0.53166	1.43347
H14	H	0.44366	0.7518	1.37123
H15	H	0.48954	0.82708	1.38068
H16	H	0.38318	0.84376	1.46791
H17	H	0.33726	0.76865	1.45825
H18	H	0.42406	0.46219	0.61025
H19	H	0.46201	0.42444	0.63161
H20	H	0.39668	0.49872	1.40809

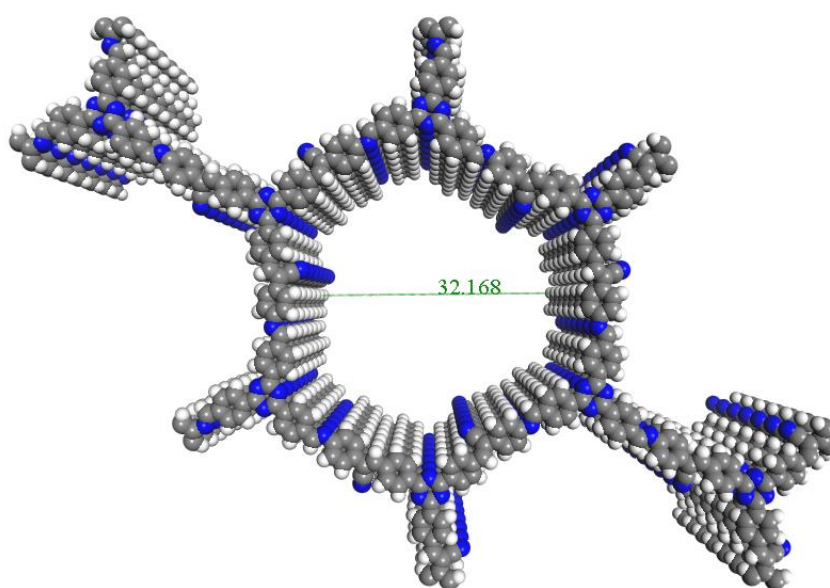


Fig. S4. Pore size of TFPT-APA COF simulated by Materials Studio.

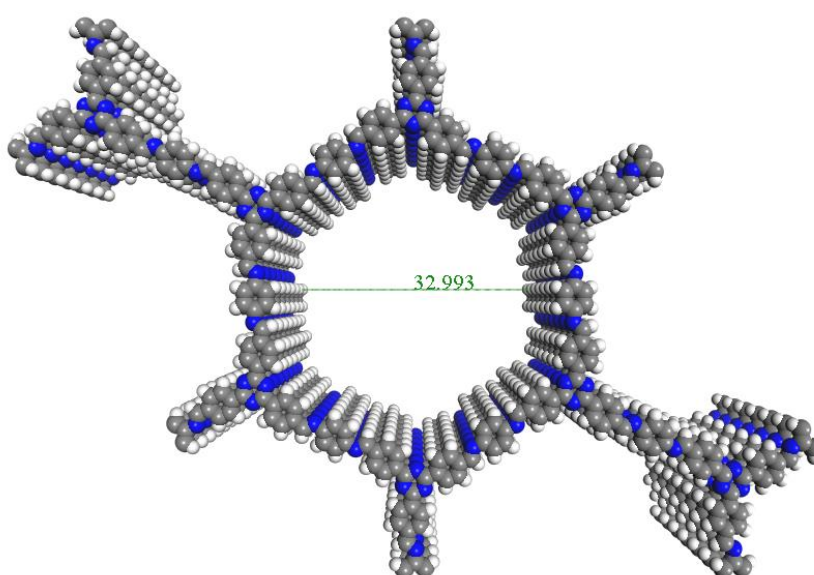


Fig. S5. Pore size of TFPT-PA COF simulated by Materials Studio.

Section S5 Characterization of COFs

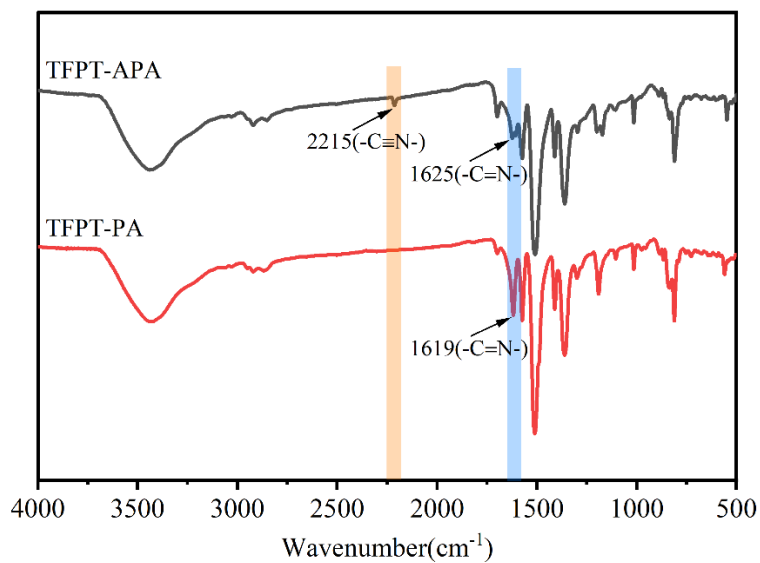


Fig. S6. FTIR spectra of TFPT-APA and TFPT-PA COF.

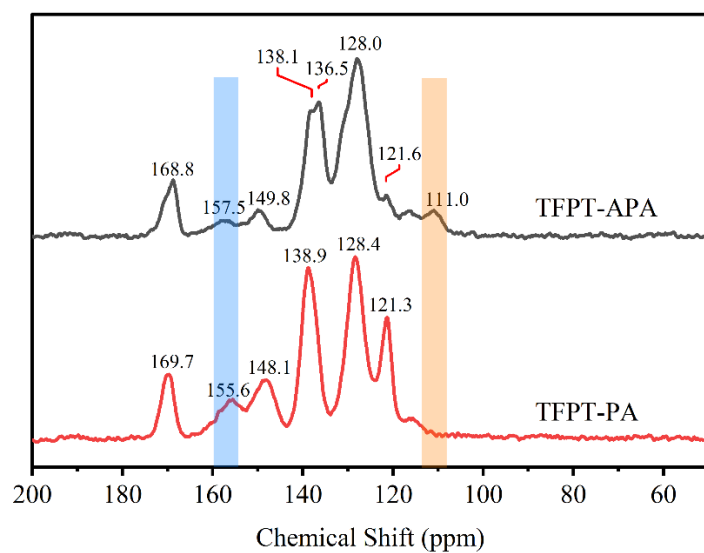


Fig. S7. ¹³C ssNMR spectra of TFPT-APA and TFPT-PA COF.

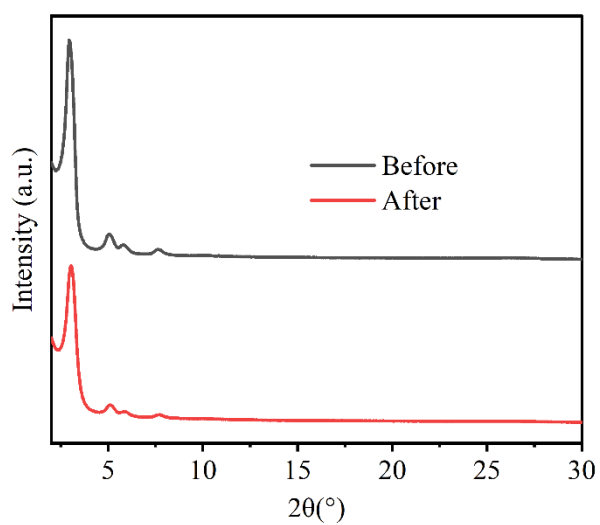


Fig. S8. XRD pattern of TFPT-APA before (black) and after (red) photocatalysis.

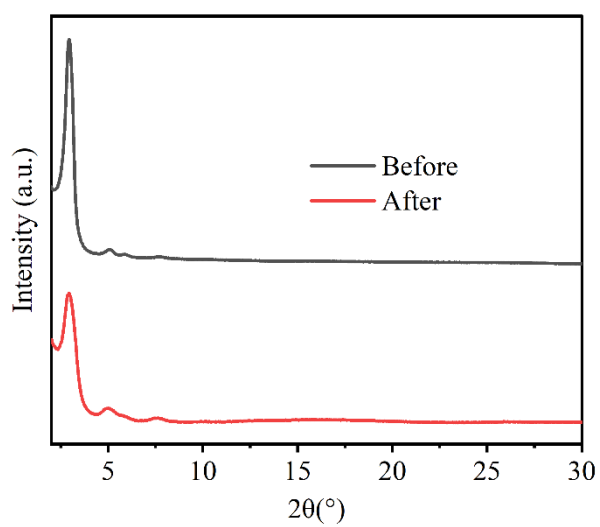


Fig. S9. XRD pattern of TFPT-PA before (black) and after (red) photocatalysis.

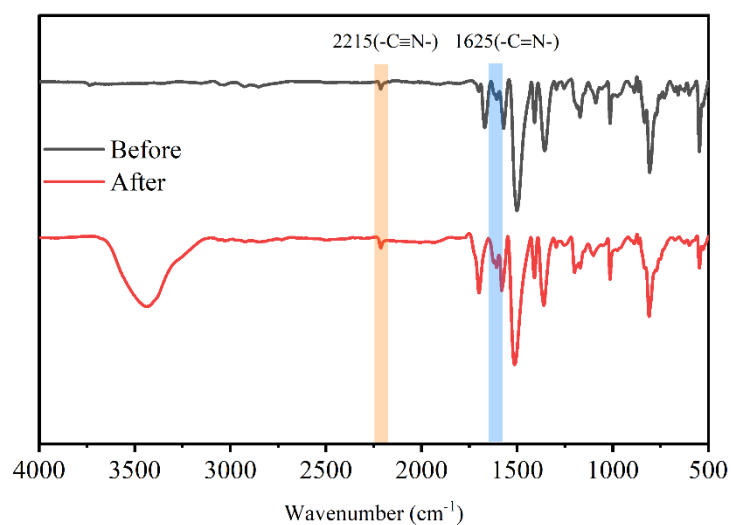


Fig. S10. FT-IR spectra of TFPT-APA before (black) and after (red) photocatalysis. The signal observed in the range of 3200 cm^{-1} to 3600 cm^{-1} corresponds to the O-H stretching vibrations of water molecules that were not completely removed after the reaction.

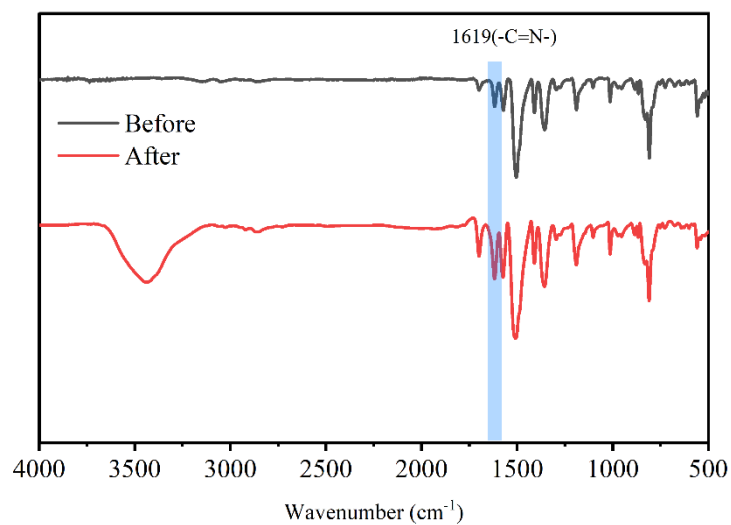


Fig. S11. FT-IR spectra of TFPT-PA before (black) and after (red) photocatalysis. The signal observed in the range of 3200 cm^{-1} to 3600 cm^{-1} corresponds to the O-H stretching vibrations of water molecules that were not completely removed after the reaction.

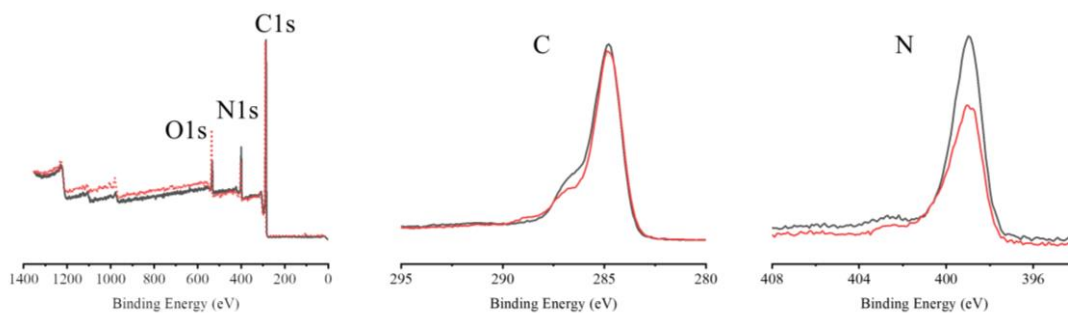


Fig. S12. XPS spectra of TFPT-APA before (black) and after (red) photocatalysis. The O1s signal could be attributed to oxygen molecules adsorbed on the sample surface from the ambient air.

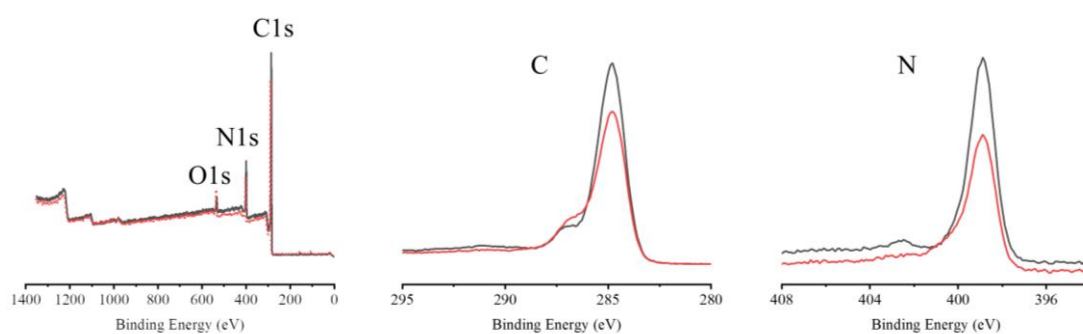


Fig. S13. XPS spectra of TFPT-PA before (black) and after (red) photocatalysis. The O1s signal could be attributed to oxygen molecules adsorbed on the sample surface from the ambient air.

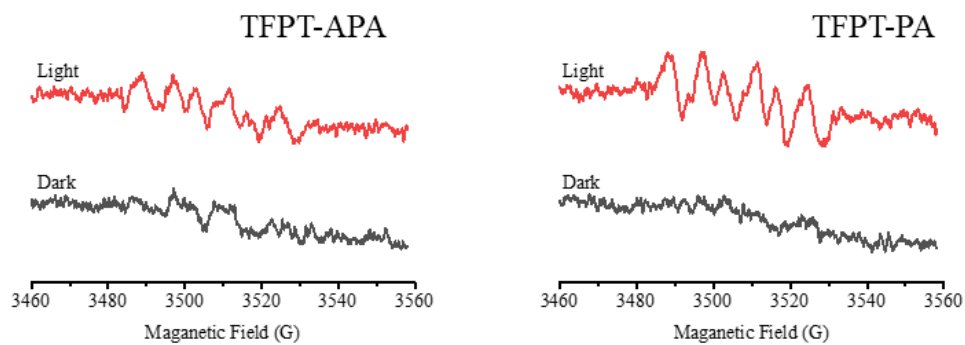


Fig. S14. ESR spectra of TFPT-APA and TFPT-PA prior to and after visible-light irradiation. DMPO: 100 mM, light source: 300 W Xenon lamp equipped with a 420 nm cutoff filter, solvent: methanol.

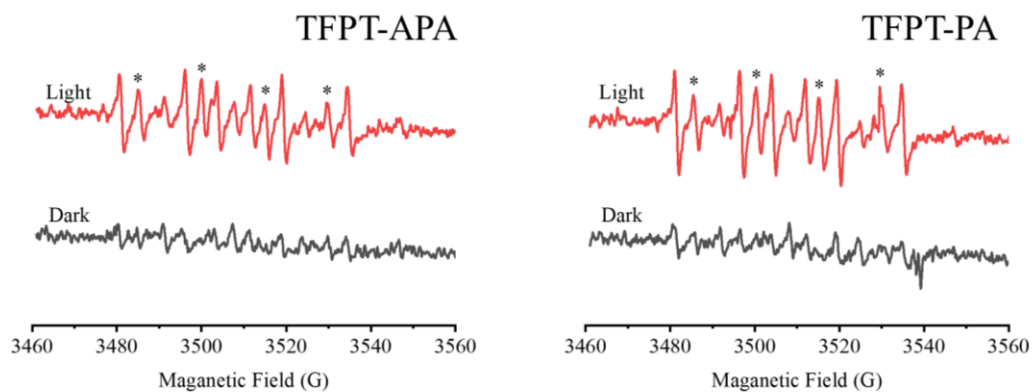


Fig. S15. ESR spectra of TFPT-APA and TFPT-PA prior to and after visible-light irradiation. The asterisked four peaks are the DMPO-OH signals. DMPO: 100 mM, light source: 300 W Xenon lamp equipped with a 420 nm cutoff filter, solvent: water.

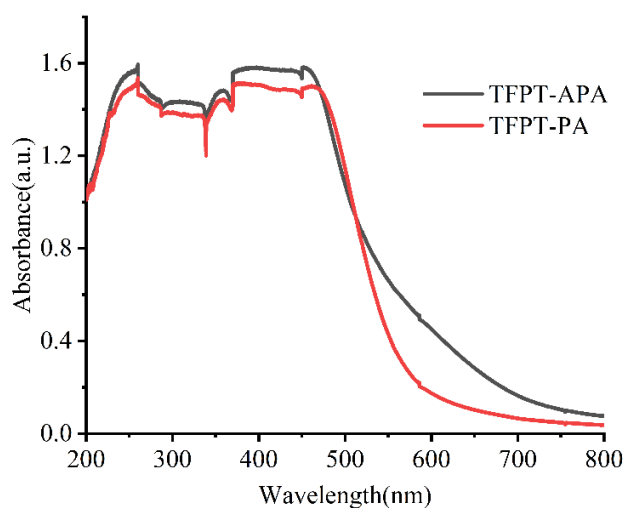


Fig. S16. UV-DRS of TFPT-APA and TFPT-PA.

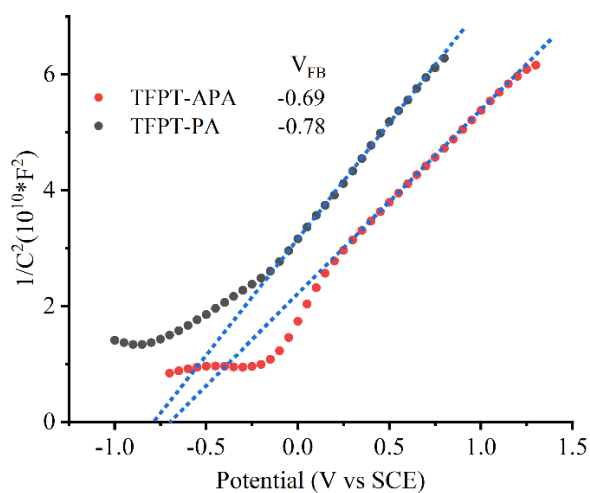


Fig. S17 Mott-Schottky plots of TFPT-APA and TFPT-PA.

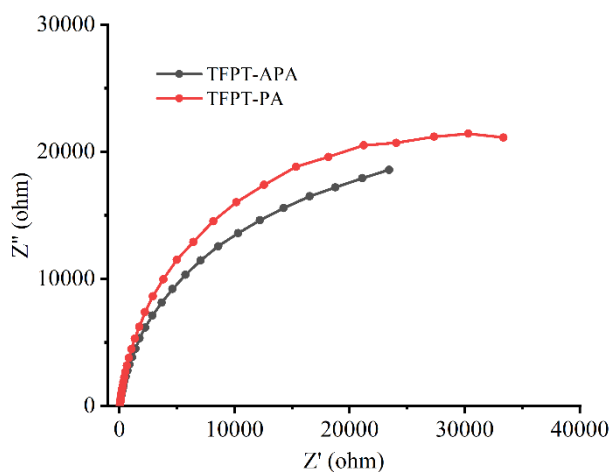


Fig. S18 EIS Nyquist plots of TFPT-APA and TFPT-PA.

Table S3 Time-resolved fluorescence fit results.

Sample	τ_1	τ_2	τ_3	B_1	B_2	B_3	τ
TFPT-APA	3.584×10^{-10}	1.652×10^{-9}	7.993×10^{-9}	0.113	0.020	0.001	1.631×10^{-9}
TFPT-PA	1.059×10^{-10}	1.712×10^{-9}	3.020×10^{-8}	0.445	0.007	0	4.315×10^{-10}

The data was fitted with using multiple exponential formulas (1). And the average decay time τ was calculated by the formula (2).

$$R(t) = B_1 e^{\frac{-t}{\tau_1}} + B_2 e^{\frac{-t}{\tau_2}} + B_3 e^{\frac{-t}{\tau_3}} \quad (1)$$

$$\tau = \frac{B_1 \times \tau_1^2 + B_2 \times \tau_2^2 + B_3 \times \tau_3^2}{B_1 \times \tau_1 + B_2 \times \tau_2 + B_3 \times \tau_3} \quad (2)$$

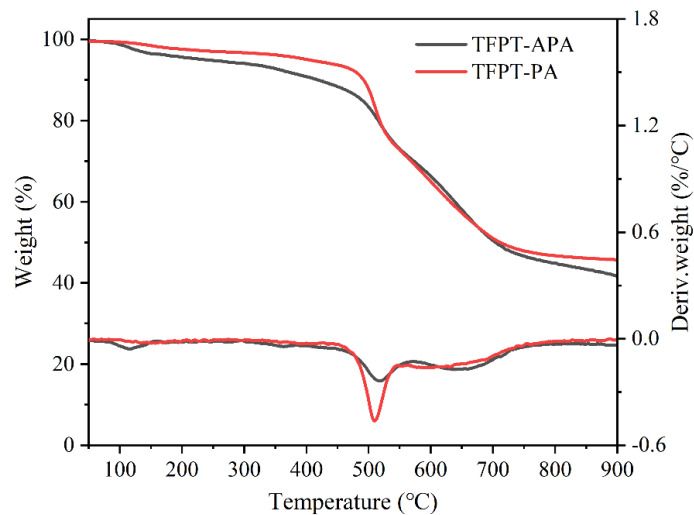


Fig. S19. TGA data of TFPT-APA COF compare with TFPT-PA COF.

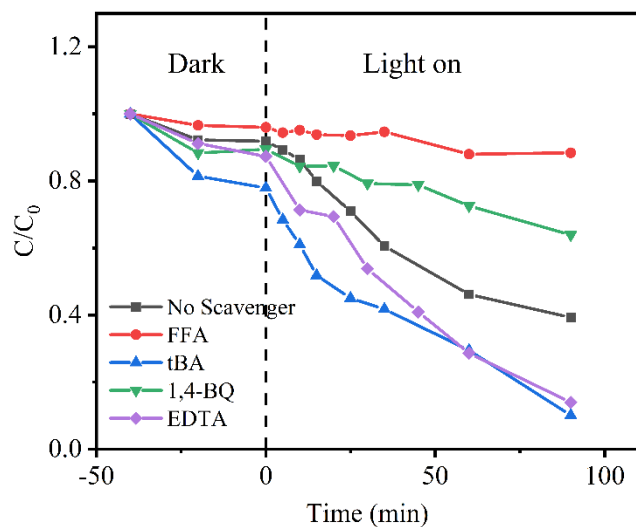


Fig. S20. Effects of FFA, tBA, 1,4-BQ, and EDTA on the photocatalytic degradation of STZ with TFPT-APA.